Volume No.07, Special Issue No.02, February 2018 www.ijarse.com

IJARSE ISSN: 2319-8354

# Influence of divalent copper substitution on the properties of nanocrystallineNi-Zn ferrites prepared by the citrategel autocombustion method

M. Siva Ram Prasad<sup>1</sup>, B.B.V.S. Vara Prasad<sup>2</sup>

<sup>1,2</sup>Department of Physics, MVGR College of Engineering (A),(India)

#### **ABSTRACT**

A series of nanocrystalline  $Ni_{0.6}Zn_{0.4-x}Cu_xFe_2O_4$  (0.00  $\leq x \leq 0.25$  in steps of 0.05) were prepared by the citrategel autocombustion method. The powders and the pelleted samples of the same composition were sintered at  $1100^{\circ}C$  for 4hrs in air atmosphere followed by natural cooling to room temperature. The powder X-ray diffraction studies indicated the formation of spinel ferrite phase while the microstructure of the samples was studied using Scanning Electron Microscopy. An improvement in the sintered density and a decrease of porosity is observed upon substitution of copper for zinc in Ni-Zn ferrite. A suitable cation distribution of all samples has been proposed based on saturation magnetization which is in well agreement with the theoretical lattice constant. Temperature variations of DC electrical resistivity measurements indicated a semiconducting nature for the samples. The changes in structural parameters are well supported by the saturation magnetization and de electrical resistivity. All the experimental observations were explained in the light of existing understanding.

Keywords: Autocombustion, Ferrite, Magnetization, Microscopy, Resistivity

#### **I.INTRODUCTION**

Since the recent past, the nanocrystalline spinel ferrites significantly attracted the scientific community owing to their importance in understanding the fundamentals of nanomagnetism, and wide range of applications such as high-density data storage, ferrofluid technology, spintronics, MRI contrast agents, magnetocalorific refrigeration, etc. [1]. Among the available spinel ferrites, current interest is on Ni-Zn ferritesbecause of their high saturation magnetization, high permeability, low coercivity, and coupled with high electrical resistivity [2] which make them an excellent choice for magnetic cores operable for frequencies upto few hundred MHz. The useful characteristics of these ferrites strongly depend on the method of preparation and the sintering conditions by large the sintering atmosphere, temperature, time and importantly the rate of cooling after sintering.

The novel wet chemical methods like co-precipitation, hydrothermal, precursors and auto combustion are advantageous compared to the conventional ceramic process for preparation of Ni-Zn ferrites since these processes are typically less time consuming with minimized evaporation losses and the obtained ferrite products are reproducible [3]. Apart from the method of processing, the properties of Ni-Zn ferrites are largely effected by the nature and amount of dopant, their valence state and the preferentially lattice site occupancy of the cations. From the past few decades various researchers worked with a view to improvise the existing properties of Ni-Zn ferrites either by employing various preparation routes and or by impurity addition [4-5].

# Volume No.07, Special Issue No.02, February 2018

www.ijarse.com

IJARSE ISSN: 2319-8354

The present study is aimed at investigating the effect of  $Cu^{2+}$  ion substitution on structural, magnetic and electrical properties of Ni-Zn ferrites suitable for Multilayer Chip Inductors (MLCI's) and surface mount devices (SMD's). The  $Cu^{2+}$  ions are remarkable as sintering aids because of their high atomic mobility, and promote interlattice diffusion of cations and thereby densification occurs at relatively lower sintering temperatures. The other advantage of copper substitution is that the sintered density and grain sizes of the ferrites specimen remainsnearly unaltered even after prolonged sintering time [6] suggesting the aptness of copper ions in the control of grain growth kinetics. It has been reported that copper substitution at higher concentration develops a liquid phase at the grain boundaries [7] which properly control the grain growth and porosity of the sample. Regarding its electronic configuration, the  $Cu^{2+}$  ion is paramagnetic with a magnetic moment of  $1\mu_B$  and usually has an octahedral site preference, but possible restitution of  $Cu^{2+}$  ions to the tetrahedral sites has been reported in many cases due to the narrow energy difference in its CFE's at the tetrahedral (A-site) and octahedral configurations (B-sites) [8].

The composition aimed in the study is Ni<sub>0.6</sub>Zn<sub>0.4-x</sub>Cu<sub>x</sub>Fe<sub>2</sub>O<sub>4</sub> (x=0.00 to 0.25 insteps of 0.05) and the autocombustion method is adopted for preparing the samples using citric acid ascomplexing or reduction agent. This method has been opted since it produces stoichiometric, ultrafine nanoparticles with homogenous particle size distribution and promotes crystallization during the synthesis. Additionally the auto-combustion synthesis is an exothermic, self-propelling chemical reaction between the salts of metal nitrates and a suitable organic fuel like urea, citric acid, PVA, etc. The key feature of this process is that the heat required to trigger the reaction is provided by the reaction itself and not from any external source [3]. Citric acid ischosen as the organic fuel in the present study owing to itsexcellent chelating characteristics as it can effectively chelatethe metal ions with varying ionic sizes and thereby preventing their selective precipitation in order to maintain compositionalhomogeneity among the constituents. Prominently,it is an effective complexing agent in producing fineferrite powder with small particle size and uniform particlesize distribution [9].

#### **II.EXPERIMENTAL DETAILS**

Primarily, required amounts of AR Grade Ni(NO<sub>3</sub>)<sub>2</sub>.6H<sub>2</sub>O, Zn(NO<sub>3</sub>)<sub>2</sub>.6H<sub>2</sub>O and Fe(NO<sub>3</sub>)<sub>3</sub>.9H<sub>2</sub>O (and Cu(NO<sub>3</sub>)<sub>2</sub>.6H<sub>2</sub>O for copper substituted samples) and C<sub>6</sub>H<sub>8</sub>O<sub>7</sub>.H<sub>2</sub>O were weighed and dissolved separately in deionized water as per the required stoichiometric proportions in order to preparea 30 gm ferrite powder. The salt solutions, with molar ratio of the metal nitrates to the citric acid is maintained at 1:1, were mixed and homogenized under vigorous stirring continuously by using a magnetic stirrer until a clear solution is formed. This mixture solution is then placed on a hot plate under constant heating and continuous stirring. When the temperature reached to about 60°C, citric acid has been added to the mixed solution dropwise under continuous stirring and constantheating. When the temperature reached to about 100°C, the solution boiled and froths appeared due to dehydration. With further increase of temperature the solution then slowly transformed to a gel. Gelation continued with elimination of water and a thickness of the gel progressively increased till a red type viscous gel is formed with evolution of reddish brown gases. The gel subsequently self-ignited, burnt and gave rise to a fleecy, massy and dry residue. The residue is ground by using an agate mortar and pestle for 1 hour to obtain a loose ferrite powder. The powders were then annealed at 1100°C for 4 hours in the usual air atmosphere

# **Volume No.07, Special Issue No.02, February 2018**

#### www.ijarse.com

IJARSE ISSN: 2319-8354

followed by natural cooling to room temperature. These annealed powders were then characterized for their structure by using Pan Analytical X'Pert Pro X-ray diffractometer with Cu-K<sub>a</sub>( $\lambda$  = 1.5418 Å) radiation at room temperature. The magnetization studies on the samples were done on a Lakeshore Vibrating Samples Magnetometer (VSM) 7410 for a maximum magnetic field of 1.5T. For density and dc electrical resistivity measurements the prepared powders have been pressed into pellets under a uniaxial pressure of 3Ton/inch<sup>2</sup> by using 15% PVA as binder. The pellets were again sintered in air atmosphere at 1100°C for 4 hours. The sintered pellets have then been ground and polished to remove any oxide layer formed on the surface of the samples. The sintered density (**d**<sub>s</sub>) of the samples was measured by using the Archimedean method and the theoretical density or X-ray density (**d**<sub>th</sub>) was calculated by using the relation in literature [10]. The surface morphology and microstructure of the samples were investigated by using a JEOL JSM 7600F Scanning Electron Microscope (SEM). The DC electrical resistivity studies on the sintered pellets were done by using the conventional two-probe method. For temperature variation of DC resistivity studies, the cell containing the sample was placed in a tubular furnace and the measurements were taken in the temperature range of room temperature to 150°C. The activation energy for conduction was determined from the slope of the logp versus 1/T plots.

#### **III.RESULTS & DISCUSSION**

#### 1.1. Powder X-Ray diffraction study

The powder XRD patterns of the Cu<sup>2+</sup> substituted Ni-Zn ferrite samples shown in Fig. 1 indicate the formation of the single phase spinel for all compositions (confirmed by using the JCPDS files [11]) with no segregated secondary phases suggesting the solubility of the cations into their respective lattice sites.

The inter-planar spacing(s) (d) were determined from the Intensity versus  $2\theta$  plot by using the Braggs law [10]. The lattice constant corresponding to each peak in the diffraction pattern was plotted against the Nelson-Riley error function  $\left(F(\theta) = \frac{1}{2} \left(\frac{\cos^2 \theta}{\sin \theta} + \frac{\cos^2 \theta}{\theta}\right)\right)$  and the accurate lattice constant (a) has been obtained from the least square fit method [10].

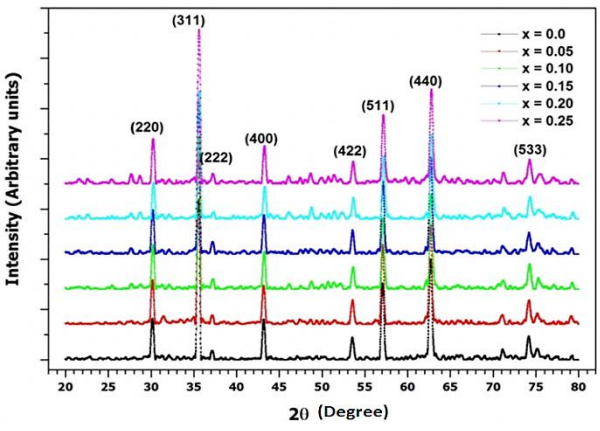


Fig.1.Powder XRD pattern of Ni<sub>0.6</sub>Zn<sub>0.4-x</sub>Cu<sub>x</sub>Fe<sub>2</sub>O<sub>4</sub>

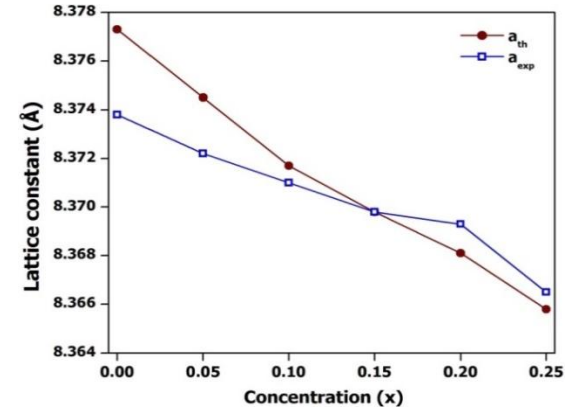


Fig.2. Lattice constant versus 'x' forNi<sub>0.6</sub>Zn<sub>0.4-x</sub>Cu<sub>x</sub>Fe<sub>2</sub>O<sub>4</sub>

# Volume No.07, Special Issue No.02, February 2018

ISSN: 2319-8354

www.ijarse.com

The lattice constant for the starting composition  $Ni_{0.6}Zn_{0.4}Fe_2O_4$  (a=8.3738 Å) is found to be in close agreement with the reported values (8.377 Å [12] & 8.3727 Å [13]) of the same composition but by a different methods of preparation [14].

The monotonic decrease in lattice constant (a)with increase in Cu<sup>2+</sup> ion substitution, shown in fig.2, is in accordance with the Vegard's law [15]. According to Vegard in the solid solution spinel within the miscibilityrange, a linear change in lattice constant with the concentration of the components is observed. The decrease in latticeconstant might be expected in the view of the fact that the substituted Cu<sup>2+</sup>ions have lower ionic radius (Å) compared to the displaced Zn<sup>2+</sup>ions (Å) [16]. Usually if the radius of the substituted ion is largerthan the displaced ion then lattice expands in order to facilitate the occupancy of the larger ion and hencelattice constant increases else the lattice constant decreases.

Usually for the Ni-Zn ferrite, the  $Zn^{2+}$ ions with free4s4p orbitals ready to form covalent bonds with the oxygen dispose them to occupy the tetrahedral sites (A), whilethe  $Ni^{2+}$ ions due to their high crystal field stabilizationenergy prefer the octahedral sites (B) whereas the  $Fe^{3+}$ ions are distributed among both A & B sites of the spinel lattice [10]. The possible cation distribution for the starting composition  $Ni_{0.6}Zn_{0.4}Fe_2O_4$  is therefore given as  $(Zn_{0.4}^{2+}Fe_{0.6}^{2+})_A[Ni_{0.6}^{2+}Fe_{1.4}^{2+}]_B$ . On substitution of  $Cu^{2+}$  for  $Zn^{2+}$  ions in Ni-Zn ferrite possible cation redistributionmight be expected due to the highly diffusive nature of copper ions which and promote an interlattice dispersal of cations [7]. Such a possibility would perpetually bring about modifications in the structural, magnetic, electric and dielectric properties of the Ni-Zn ferrites with inclusion of copper into spinel lattice. The occupancy of the  $Cu^{2+}$  ions at the A and B-sites of the spinel lattice is arrived based on the saturation magnetization (M<sub>s</sub>) using VSM. The experimental Bohr magneton values were determined for each composition of Ni-Cu-Zn ferrite and subsequently theoretical Bohr magneton value was calculated by adjusting the ratios of  $Cu^{2+}$  and  $Fe^{3+}$ occupying the A & B-sites until an appropriate distribution is arrived. Subsequently the theoretical lattice constant (a<sub>th</sub>) for each composition of Ni-Cu-Zn ferrite was computed for substantiation of the proposed cation distribution.

Aappropriatecation distribution for each composition of Ni-Cu-Zn ferriteis represented in table-1 and the theoretical lattice constant  $(a_{th})$  has been determined by using the expression  $[10]_{,a_{th}} = \frac{8}{3\sqrt{3}} \left[ (r_A + R_O) + \sqrt{3}(r_B + R_O) \right]$ . Where  $r_A \& r_B$  are the average cation radius at the A and B-sites respectively and Ro is the radius of the oxygen anion. The following are the radius of the ions [17] involved in determination of  $r_A$ ,  $r_B \& a_{th}$ ; tetrahedral configuration:  $(r_{Zn^2+} = 0.60 \text{Å}; r_{Cu^2+} = 0.57 \text{Å}; r_{Fe^3+} = 0.49 \text{Å})$  and for the octahedral configuration:  $(r_{Ni^2+} = 0.69 \text{Å}; r_{Cu^2+} = 0.73 \text{Å}; r_{Fe^3+} = 0.645 \text{Å})$  and  $R_O = 1.38 \text{Å}$ .

Table 1: Cation distribution, r<sub>A</sub>&r<sub>B</sub> and the u-parameter for Ni<sub>0.6</sub>Zn<sub>0.4-x</sub>Cu<sub>x</sub>Fe<sub>2</sub>O<sub>4</sub>

x	Cation distribution	$r_A(A)$	$r_B(A)$	a <sub>th</sub> (Å)	u
0.00	$(Zn_{0,4}^{2+}Fe_{0,6}^{3+})[Ni_{0,6}^{2+}Fe_{1,4}^{3+}]$	0.5340	0.65850	8.3773	0.381912
0.05	$(Zn_{0.35}^{2+}Fe_{0.65}^{3+})[Ni_{0.6}^{2+}Cu_{0.05}^{2+}Fe_{1.35}^{3+}]$	0.5285	0.66062	8.3745	0.381547
0.10	$(Zn_{0.30}^{2+}Fe_{0.70}^{3+})[Ni_{0.6}^{2+}Cu_{0.10}^{2+}Fe_{1.30}^{3+}]$	0.5230	0.66275	8.3717	0.381179

# Volume No.07, Special Issue No.02, February 2018

#### www.ijarse.com

0.15	$(Zn_{0.25}^{2+}Cu_{0.07}^{2+}Fe_{0.68}^{2+})[Ni_{0.6}^{2+}Cu_{0.08}^{2+}Fe_{1.32}^{2+}]$	0.5231	0.66190	8.3698	0.381219
0.20	$(Zn_{0.20}^{2+}Cu_{0.14}^{2+}Fe_{0.66}^{2+})[Ni_{0.6}^{2+}Cu_{0.06}^{2+}Fe_{1.34}^{2+}]$	0.5232	0.66105	8.3681	0.381258
0.25	$(Zn_{0.15}^{2+}Cu_{0.21}^{2+}Fe_{0.64}^{3+})[Ni_{0.6}^{2+}Cu_{0.04}^{2+}Fe_{1.36}^{3+}]$	0.5233	0.66020	8.3658	0.381298

A close agreement between the experimental (a) and theoretical  $(a_{th})$  lattice constant values (fig.2) advocates that (i) the proposed cation distribution might be the correct one with copper ions occupying only the B-sites of the spinel lattice only uptoa substitution level of 5mol% (x $\leq$ 0.10) and at higher concentrations migration of the copper ions to the A-sites in substantial amounts. (ii) byadoptingthe nitrate-citrate gel autocombustion method ultrafine Ni-Zn ferrite powders have been produced which when annealed/sintered no appreciable deviation form stoichiometry is observed.

The oxygen positional parameter (u), which depends on the radius ratio of the tetrahedral and octahedral cation radii, has been obtained by the formula available in the literature [18] and represented in table-1. The significant decrease in the u-parameter up to x=0.10 level of copper substitution clearly indicates a contraction of AO<sub>4</sub>tetrahedra in the <111> direction due to removal of the larger divalent zinc ions at the A-sites though being replaced by the smaller ferric ions in identical amounts. At higher substitution levels (x>0.10) a gradual increase in the u-parameter is seen due to the migration of copper ions in increasing amounts from the B to A-sites and displacement of the Fe<sup>3+</sup> ions in equal amounts to the B-sites. Such a possibility might have resulted in compression of the BO<sub>6</sub>octahedra and subsequent expansion of the AO<sub>4</sub>tetrahedra in-order to adjust the differences in ionic radii of the redistributing Cu<sup>2+</sup> and Fe<sup>3+</sup> ions between the two interstitial configurations. Therefore the ratio between the tetrahedral and octahedral average cation radius increases for x>0.10 level of copper substitution and hence theu-parameter which is proportional to this ratio also increases.

#### 1.2. Density and microstructural studies

The variation of sintered density  $(d_s)$ , X-ray density  $(d_x)$  and the percentage of porosity (P) for the Ni-Cu-Zn ferrite system (fig.3.) is attributed to the role of copper ions during sintering and the density differences between the substituents.

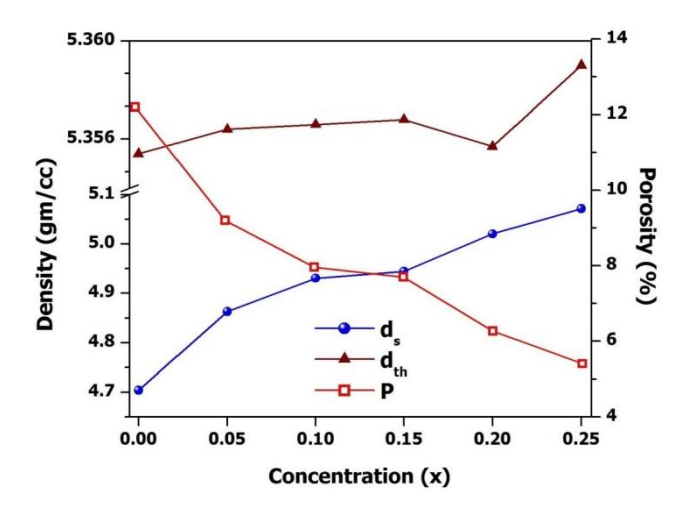


Fig.3. Sintered density (d<sub>s</sub>), X-Ray density (d<sub>th</sub>) and Porosity (P%) for Ni<sub>0.6</sub>Zn<sub>0.4-x</sub>Cu<sub>x</sub>Fe<sub>2</sub>O<sub>4</sub>

ISSN: 2319-8354

# Volume No.07, Special Issue No.02, February 2018 www.ijarse.com

IJARSE ISSN: 2319-8354

The increase in the sintered density  $(d_s)$  might be due to the augmentation of sintering mechanism due to the presence of the  $Cu^{2+}$  ions having high atomic mobility compared to that of  $Ni^{2+}/Zn^{2+}/Fe^{3+}$  ions. Presence of ions like  $Cu^{2+}$  in the spinel lattice would easily result in highly dense ceramic microstructures at relatively lower sintering temperatures and times. Divalent copper ions having high atomic mobility and excellent solid state solubility when enter the spinel lattice, promotes lattice diffusion by increasing the diffusion paths for the other cations. As discussed by Gupta & Coble [19], the intensification in the diffusion paths during sintering leads to the increase in the rate of intercation diffusion through the lattice which yields a dense solid state solution. Also the density of the substituted copper (8.96 g/cc) is relatively higher than the displaced zinc (7.13 g/cc) and hence the observed increase in the experimental density with copper substitution follows the density difference of the individual elements.

The higher X-ray or the theoretical density  $(d_x)$  for the Ni-Cu-Zn ferrites (fig.3) compared with the experimental density  $(d_s)$  is expected as the sintered specimen contains cracks and pores on the macroscopic scale and vacancies on the atomic scale and thus determining the density experimentally involves these defects. The X-ray density  $(d_{th})$  on the other hand is just the ratio of the weight of atoms in unit cell and the volume of the unit cell and is determined precisely by measuring the lattice parameter. Therefore the measurement of the X-ray density does not involve any macro or microscopic defects. A slight increase in X-ray density (fig.4) indicates that the decrease in the molecular weight of the Ni-Cu-Zn ferrite is relatively slower than the corresponding decrease in lattice constant with the increase of copper.

The percentage of porosity (P%) with Cu<sup>2+</sup> ion substitution (fig.3) shows an opposite trend to the sintered density. Customarily the total porosity in ferrite ceramics has contributions both from the intra-granular and inter-granular pores depending on whether the pores principally reside at the grain boundaries or the trapped within the grains respectively. The pores at the grain boundaries are never damaging but those trapped within the grains causes severe detrimental effects to the magnetic and mechanical properties of the polycrystalline ferrites. The intra-granular porosity is virtually impossible to eliminate and appears when the grain growth rate is very high due to excessively high sintering temperature, prolonged sintering timeand at low oxygen partial pressure in the sintering atmosphere [20]. The observed significant decrease in pore concentration with copper substitution in Ni-Zn ferrite is well agreement with the increase of sintered density as highly dense ferrites samples always prefer a uniform microstructure with small grains and narrow size distribution with pores only residing at the grain boundaries.

The SEM micrographs shown in figure.4 suggests a clear modification in the microstructure of Ni-Zn ferrite with copper substitution chiefly in terms of grain size, size distribution of grains, shape of the grains and grain boundaries. Out of the grain size and porosity of microstructures, the grain size is more important parameter affecting the magnetic properties of ferrites. Grain growth is closely related to the grain boundary mobility and the grain amalgamation in which the smaller grains surrounding a bigger grain coalesce taking the advantage of the available thermal energy during sintering.

The mean grain size for all Ni-Cu-Zn ferrite compositions, determined by using the linear intercept method [21], showed an increase upto x=0.15 level of copper substitution and the microstructural development is also noticed to be well homogeneous in this substitution range.

Volume No.07, Special Issue No.02, February 2018 www.ijarse.com

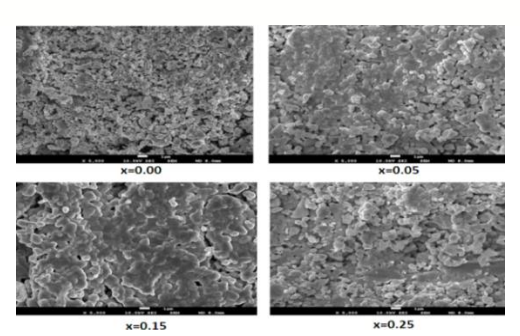


Fig.4. SEM micrographs of Ni<sub>0.6</sub>Zn<sub>0.4-x</sub>Cu<sub>x</sub>Fe<sub>2</sub>O<sub>4</sub>

The microstructure of the un-substituted Ni-Zn ferrite (fig.4& x=0.00) is noticed to contain mostly polyhedral shaped grains and a few pyramidal shaped but distributed randomly. No clear formation of the grain boundaries has been perceived and size distribution of the grains is noticed to be random. The mean grain size for x=0.00 is found to be 2.23 µm. The micrographs with increase of copper substitution (fig.4& for x=0.05; x=0.15) indicate that the grain growth rate is normal with a significant increase in the grain size from 3.05 to 4.18µm. Generally in ceramic microstructures like the ferrites the grain growth occurs via the grain boundary motion and or by the grain coalescence. Also the grain boundaries separating the grains are noticeably well observed. The shapes of the grains are largely polyhedral with a few spherical and other shapes. The observed increase in the grain growth with copper incorporation could again be well related to the beneficiary characteristics of the Cu2+ ions as a sintering aid which improvises the diffusion paths and accelerate the interdiffusion of cations in the solid solution [6]. Usually for a spinel solid solution the diffusion rate of cationic and anionic species through the available volumeof the solid is greatly enhanced by the lattice defects in particular vacancies. The pores play the role of vacancy sources while the grain boundaries act as vacancy sinks. The sintering mechanism involves the creation of vacancies at the curved surfaces of the pores and their transport through the grains via the diffusion of ionic species and absorption of pores at the grain boundaries[20]. During the sintering, the available thermal energy generates a force that drives the grain boundaries to grow over pores, thereby decreasing the pore volume and making the material dense [7]. From the microstructure it is also evident that the porosity upto x=0.15 level of copper substitution is principally intergranular.

The grain growth behavior in polycrystalline ceramics is considered as the struggle between the driving force for grain boundary movement i.e. the thermal energy and the retarding force exerted by pores. The pores usually contain trapped gases and the internal pressure of the gases always resists in motion. The grain growth, being a result of interparticle mass transport, appears to be dominated by the bimodal diffusion mechanism [7], lattice and grain boundary diffusion. When the driving force for the grain boundary of each grain is homogeneous, the sintered body attains a uniform grain size distribution. For higher concentrations of  $Cu^{2+}$  substitution (x=0.25) the grain growth is noticed to be inhibited involving a recrystallization process. Such a decrease in the grain size for higher concentrations of  $Cu^{2+}$  substitution has been reported in Ni-Zn ferrites previously but of a different composition and different method of preparation [22]. Apart from the copper the substitution of  $Ti^{4+}$ ,  $Cd^{2+}$  and  $Zn^{2+}$  ions also displayed a similar microstructural behavior in various mixed ferrite systems [23].

ISSN: 2319-8354

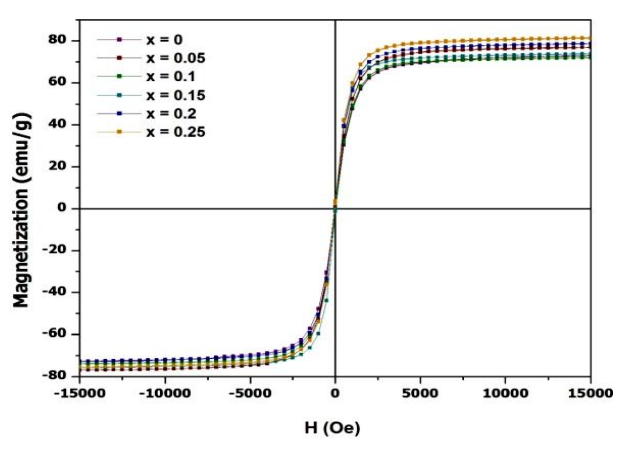
# Volume No.07, Special Issue No.02, February 2018

#### www.ijarse.com

#### IJARSE ISSN: 2319-8354

#### 1.3. Magnetization studies

Figure.5 display the room temperature M-H loops for the Ni-Cu-Zn ferrite samples which are magnetized to saturation and the narrowness of the hysteresis loops is a characteristic of the soft ferrites. The observed variation in room temperature saturation magnetization (fig.6) with the increase of copper substitution can be explained based on (i) the modification of predominant exchange interactions between the cations; (ii) substitution of paramagnetic  $Cu^{2+}$  ions for the diamagnetic  $Zn^{2+}$ ; (iii) cation redistribution in the spinel lattice due to substitution of copper ions.



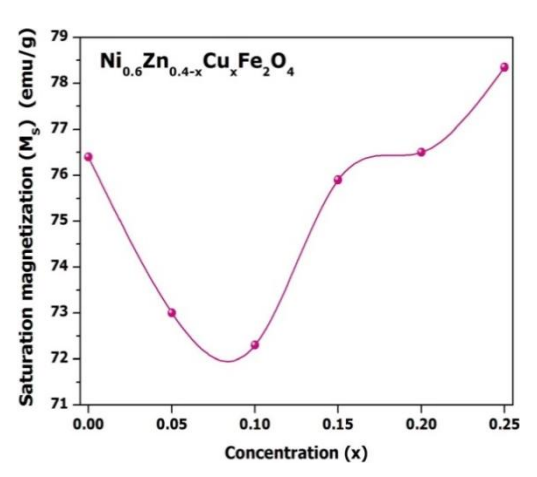


Fig.5. M-H loops of Ni<sub>0.6</sub>Zn<sub>0.4-x</sub>Cu<sub>x</sub>Fe<sub>2</sub>O<sub>4</sub>

Fig.6.M<sub>s</sub> versus 'x'

According to Neel [24], among the three exchange interactions (A-A, B-B & A-B) that prevail among the cations in the spinel lattice the A-B exchange interaction is predominant which aligns the spin magnetic moments of the cations on the A and B-sublattices antiparallel and the resulting magnetic moment of the spinel lattice is therefore the difference between the magnetic moments of A and B- sublattices. The A-B exchange interaction strength always depends on nature of the magnetic ions, the magnetic moments of the cations and their distribution in the spinel lattice and the distances between the magnetic ions.

The observed in initial decrease in saturation magnetization upto x=0.10 level (fig.6) of  $Cu^{2+}$  ion substitution is ascribed to the preferential occupancy of copper ions to the B-sites and simultaneous migration of Fe<sup>3+</sup> ions to the A-sites in equal amount in order to occupy the vacant sites created by the removal of zinc at the A-sub lattice. The possible cation distribution for  $Ni_{0.6}Zn_{0.4-x}Cu_xFe_2O_4$  for  $x\leq 0.10$  is therefore represented as  $(Zn_{0.4-x}^2Fe_{0.6+x}^2)[Ni_{0.6}^{2+}Cu_x^2+Fe_{1.4-x}^{2+}]$ . Such a possibility would decrease the B-sublattice magnetic moment while the A-sublattice magnetic moment observes an increase due to dissimilarity in the magnetic moments of the cations. The ferromagnetic  $Fe^{3+}$  and  $Ni^{2+}$  ions have a moment of  $3\mu_B$  2  $\mu_B$  respectively while the paramagnetic  $Cu^{2+}$  has a moment of  $1\mu B$ . The net magnetic moment of the spinel lattice which is just the difference between magnetic moments of the B and A-sublattices therefore decreases and hence the observed saturation magnetization.

For x=0.15 to 0.25, the observed increase in saturation magnetization is due to possible influx of the  $Cu^{2+}$  ions to the tetrahedral sites in increasing amounts and migration of equal amounts of  $Fe^{3+}$  ions to the B-sites. This results not only an upsurge in magnetic moment difference between the A & B-sites but also modifies largely

# Volume No.07, Special Issue No.02, February 2018 www.ijarse.com

IJAKSE ISSN: 2319-8354

the prevailing exchange interactions in a positive direction. The rearrangement of cations for x=0.15 to 0.25 substitution levels of  $Cu^{2+}$  is represented as,  $(Zn_{0.4-x}^{2+}Cu_z^{2+}Fe_{0.6+x-z}^{2+})[Ni_{0.6}^{2+}Cu_{x-z}^{2+}Fe_{1.4-x+z}^{2+}]$ .

Such a reordering might be expected to strengthen the super-exchange interactions by understanding the AB<sub>2</sub>O<sub>4</sub> spinel configuration. In such configuration, a cation at the A-site is surrounded by 12 B-site nearest neighboring cations while a B-site cation is surrounded by 6 nearest neighboring A-site cation for sizeable A-B exchange interaction [25]. Immigration of Cu<sup>2+</sup> ions to the A-sites would develop additional A-B interactions of the form  $\mathbf{F}e^{\mathbf{2}+} - \mathbf{0}^{\mathbf{2}-} - \mathbf{C}u^{\mathbf{2}+}$ ,  $\mathbf{C}u^{\mathbf{2}+} - \mathbf{0}^{\mathbf{2}-} - \mathbf{N}i^{\mathbf{2}+} & \mathbf{C}u^{\mathbf{2}+} - \mathbf{0}^{\mathbf{2}-} - \mathbf{F}e^{\mathbf{3}+}$  and also weakly paramagnetic  $\mathbf{C}u^{\mathbf{2}+} - \mathbf{0}^{\mathbf{2}-} - \mathbf{C}u^{\mathbf{2}+}$  interaction apart from the already existing strongly ferromagnetic  $\mathbf{F}e^{\mathbf{3}+} - \mathbf{0}^{\mathbf{2}-} - \mathbf{F}e^{\mathbf{3}+}$  and  $\mathbf{F}e^{\mathbf{3}+} - \mathbf{0}^{\mathbf{2}-} - \mathbf{N}i^{\mathbf{2}+}$  interactions in the pristine Ni<sub>0.6</sub>Zn<sub>0.4</sub>Fe<sub>2</sub>O<sub>4</sub>. Therefore the overall super-exchange interaction strength increases with migration of Cu<sup>2+</sup> to the A-sites of the spinel lattice and consequently the observed rise in the saturation magnetization above x>0.10, while the theoretical value is computed from the cation distribution and represented in table-2.

Table-2: Molecular weight, experimental and theoretical Bohr magneton (μ)number for Ni<sub>0.6</sub>Zn<sub>0.4-x</sub>Cu<sub>x</sub>Fe<sub>2</sub>O<sub>4</sub>

		= " " "			
x	Molecular weight (amu)	$\mu_{\mathrm{exp}}$	$\mu_{\mathrm{th}}$		
0.00	237.0718	$3.2430~\mu_B$	3.60 µ <sub>B</sub>		
0.05	236.9796	$3.0975\;\mu_B$	3.35 μ <sub>B</sub>		
0.10	236.8874	$3.0666~\mu_B$	3.10 μ <sub>B</sub>		
0.15	236.7952	$3.2180~\mu_B$	3.13 μ <sub>B</sub>		
0.20	236.7030	$3.2422~\mu_B$	3.16 μ <sub>B</sub>		
0.25	236.6108	$3.3193~\mu_B$	3.19 μ <sub>B</sub>		

Also, the variation in the experimental number of Bohr magneton per formula unit of Ni-Cu-Zn is noticed to be in close concurrence (Table-2) with the theoretical value which supports the proposed cation distribution further. The experimental number of Bohr magnetons is obtained from the formula  $\mu_{exp} = \frac{M_s W}{5585} \mu_B$  [26], where  $M_s$  is the experimental saturation magnetization, W is the molecular weight of the Ni-Cu-Zn ferrite composition. The theoretical number of Bohr magnetons is obtained from the cation distribution and are strictly valid at 0K by considering the spin moments on the A and B-sublattices aligned exactly antiparallel and thereby slightly higher compared to the experimental value. But the experimental value determined from the saturation magnetization measured at room temperature which the magnetic spins on the A and B-sites may not be truly antiparallelas an effect of temperature.

#### 1.4. DC electrical Resistivity studies

The electrical conductivity in ferrites is accredited to the Verwey–deBoer mechanism of hopping of the charge carriers between ions of the same elements but in different valence states and distributed randomly among the available crystallographic lattice sites [27]. The presence of the ions in different valence states is attributed to the sintering mechanism.

# Volume No.07, Special Issue No.02, February 2018 www.ijarse.com

IJARSE ISSN: 2319-8354

Generally for a stoichiometric Ni–Zn ferrite with normal site preference of cations, the Ni<sup>2+</sup>ions preferentially occupy the octahedral B-sites and the Zn<sup>2+</sup> ions populate the tetrahedral A-sites whereas the Fe<sup>3+</sup> ions are distributed among the A and B-sites. On sintering the Ni–Zn ferrite at elevated temperatures, volatilization of zinc fractional amounts introduce possiblecation vacancies and unsaturated oxygen ions. The excess electrons then bond with neighboring Fe<sup>3+</sup> ions due to electrostatic interaction and thereby generate the Fe<sup>2+</sup> ions. The volatilization of zinc is represented as,  $Zno \rightarrow Zn + \frac{1}{2}O_2[28]$ . Now, the overall charge balance of the spinel lattice is consequently restored by the oxygen loss from the sample which may lead to slight deviation from stoichiometry. The number of Fe<sup>2+</sup> ions formed depends on the amount of zinc distilled out from the sample which inherently depends on the sintering time and temperature. Possible formation of Ni<sup>3+</sup> ions occur during the cooling cycle due to substantial absorption of oxygen in the oxygen rich regions of the sample [29].

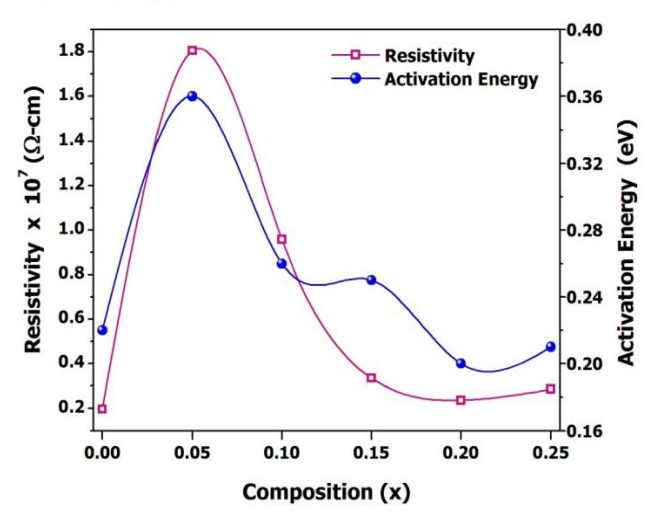
The occurrence of these ions in more than one valence state would generate the conduction paths  $Fe^{2+} \leftrightarrow Fe^{2+} + e^-$  and  $Ni^{2+} \leftrightarrow Ni^{2+} + e^+$  for hopping of electrons and holes respectively. The probability of hopping largely depends on the distance between the cations involved and is associated with activation energy (E<sub>a</sub>) which is the energy barrier associated by the charges during hopping. In the spinel structure, based on the distances between the cations the hopping of charges between the cations on the B-sites is more predominant than those between A and B sites and the hopping between the A-site cations can be neglected owing to their larger separation and also the Fe<sup>2+</sup> ions formed during sintering fondly occupy the B-sites of the spinel lattice only.

The room temperature dc electrical resistivity (fig.7) exhibited an initial increase at x = 0.05 level of  $Cu^{2+}$ substitution and thereafter a gradual decrease in resistivity is observed at higher concentrations (for x= 0.10 to 0.25). The initial increase might be related to the preferential site occupancy of Cu<sup>2+</sup> ions to the octahedral sites which regulate the charge hopping by blocking the conduction paths of  $Fe^{2+} \leftrightarrow Fe^{3+}$  and  $Ni^{2+} \leftrightarrow Ni^{3+}$  but at higher concentrations, the insurgence of the Cu<sup>2+</sup> ions to the A-sites of the lattice and migration of Fe<sup>3+</sup> ions in equal amounts to the B-sites improvise the electric conduction via Fe<sup>2+</sup>  $\leftrightarrow$  Fe<sup>3+</sup>. Such a sudden increase in the resistivity for the initial substitution level of Cu<sup>2+</sup> has been previously reported in another mixed ferrite system and of a different composition [30]. Also the increase in the mean grain size might possibly increase the conduction through the grains and lessen the scattering at the grain boundaries. The depletion of Zn<sup>2+</sup> ions from the lattice due to substitution of Cu2+ also contributes to the observed decrease in resistivity as the as the polycrystalline ferrites with zinc content are well known to improve the resistivity [31]. The decrease in dc electrical resistivity for higher concentrations of  $Cu^{2+}$  (i.e for x>0.05) can also be linked to the swift decrease in the porosity with copper substitution. This is because the pores act as electron scattering centers and invariably introduce the insulating or impeding paths to the electrons and result in increase of electrical resistivity. Also the pores at the grain boundaries lessen the individual grain to grain contact area and thus results in decrease of conductivity through the grains [32].

Volume No.07, Special Issue No.02, February 2018

#### www.ijarse.com

IJARSE ISSN: 2319-8354



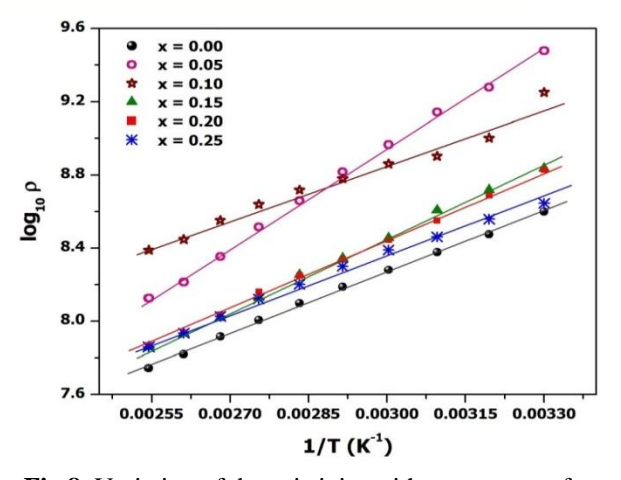


Fig.7. DC resistivity of Ni<sub>0.6</sub>Zn<sub>0.4-x</sub>Cu<sub>x</sub>Fe<sub>2</sub>O<sub>4</sub>

**Fig.8.** Variation of dc resistivity with temperature for Ni<sub>0.6</sub>Zn<sub>0.4-x</sub>Cu<sub>x</sub>Fe<sub>2</sub>O<sub>4</sub>

The variation of dc electrical resistivity with temperature (fig.8) for the Ni-Cu-Zn ferrite can be represented by the Arrhenius expression  $\rho_t = \rho_0 e^{\frac{E_g}{K_g T}}$  [26], where  $\rho_t$  is the electrical resistivity at temperature T Kelvin,  $\rho_o$  is the pre-exponential constant,  $K_B$  is the Boltzmann constant and T is the absolute temperature. Figure 8specifies that the copper substituted Ni-Zn ferrite samples exhibit semiconducting characteristics as it is usually occurs in ferrites and the activation energy ( $E_a$ ) for conduction is obtained from the slope of the straight line graph of logp versus 1/T. In ferrites, the electrons are localized as there is little overlap betweenthe wavefunctions of ions situated on the adjacent sites. The ions occasionallycome closer due to lattice vibrations and the transfer of electrons among the ions situated on the adjacent sites occurs with high probability. Such a transfer of charge is characterized an activation energy ( $E_a$ ) and therefore making the mobility of the charge carriers temperatured ependent [32]

The variation in the activation energy for the specimen in the present study is in well accordance with the observed variation with electrical resistivity indicating that ferrites with high resistivity possess higher activation energies for charge hopping. The observed activation energies in the range of 0.21eV to 0.36eV indicate a possible electron hopping mechanism.

#### **IV.CONCLUSIONS**

The powder X-Ray diffraction patterns of all the Ni-Cu-Zn ferrite samples displayed a single phase spinel structure indicating the solubility of the cations into the spinel lattice. The observed modification in the structure of Ni-Zn ferrite upon copper substitution is attributed to the difference in the ionic radius of the substituted Cu<sup>2+</sup> and displaced Zn<sup>2+</sup> ions and also to the redistribution of cations. The increase in experimental density and decline of porosity is reflected in the SEM micrographs wherein the copper ions promoted a homogenous microstructure in terms of grain size and size distribution. The variation in the saturation magnetization and dc electrical resistivity is attributed to the role of Cu<sup>2+</sup> ions and its occupancy to the preferential lattice sites. In conclusion, the prepared nanocrystalline Ni-Cu-Zn ferrites possess higher magnetization, dc resistivity and sintered density even for lower sintering temperatures making them suitable for MLCI applications.

# Volume No.07, Special Issue No.02, February 2018 www.ijarse.com

#### IJARSE ISSN: 2319-8354

#### **REFERENCES**

- [1] Sangeetha Thakur, S.C. Katyal, A. Gupta, V.R. Reddy, S.K. Sharma, M. Knobel, and M. Singh, Nickel-Zinc Ferrite from Reverse Micelles Process: Structural and Magnetic Properties, Journal of Physical Chemistry C 113(49), 2009, 20785-20794.
- [2] M.S.R. Prasad, B.R. Babu, K.V. Ramesh and K. Trinath, DC electrical resistivity studies and structure of Ni<sub>0.5</sub>Zn<sub>0.5</sub>CrxFe<sub>2-x</sub>O<sub>4</sub>nanoferrites, International Journal of Modern Physics B 29(16), 2015, 1550101 (1-16).
- [3] M.S.R. Prasad, B.R. Babu, K.V. Ramesh and K. Trinath, Structural and Magnetic Studies on Chromium Substituted Ni-Zn Nano Ferrite Synthesized by Citrate Gel Auto Combustion Method, Journal of Superconductivity and Novel Magnetism 27(9), 2014, 2735-2745.
- [4] B.R. Babu, B.B.V.S. Prasad and M.S.R. Prasad, Study of electrical and magnetic properties of Ni-Zn-Mg ferrite system, Modern Physics Letters B 28(31), 2014, 1450244 (1-10).
- [5] K.M. Batoo and M.S. Ansari, Low temperature-fired Ni-Cu-Zn ferrite nanoparticles through auto-combustion method for multilayer chip inductor applications, Nanoscale Research Letters 7, 2012, 112.
- [6] E. Rezlescu, L. Sachelarie, P.D. Popa and N. Rezlescu, Effect of substitution of divalent ions on the electrical and magnetic properties of Ni-Zn-Me ferrites, IEEE Transactions on Magnetics 36 (6), 2000, 3962-3967.
- [7] M. ManjurulHaque, M. Huq and M.A. Hakim, Influence of CuO and sintering temperature on the microstructure and magnetic properties of Mg-Cu-Zn ferrites, Journal of Magnetism and Magnetic Materials 320 (21), 2008, 2792-2799.
- [8] G.F. Goya, H.R. Rechenberg and J.Z. Jaing, Structural and magnetic properties of ball milled copper ferrite, Journal of Applied Physics 84(2), 1998, 1101.
- [9] A. Sutka,, and G. Mezinskis, Sol-gel auto-combustion synthesis of spinel-type ferrite nanomaterials, Frontiers of Materials Science 6(2), 2012, 128-141.
- [10] M.S.R. Prasad, B.B.V.S. Prasad, B.R. Babu, K.H. Rao, and k.V. Ramesh, Magnetic properties and DC electrical resistivity studies on cadmium substituted nickel-zinc ferrite system, Journal of Magnetism and Magnetic Materials 323, 2011, 2115-2121.
- [11] JCPDS Files Card # 08-0234.
- [12] D.V. Kurmude, R.S. Barkule, A.V. Raut, D.R. Shengule and K.M. Jadhav, X-ray diffraction and cation distribution studies in zinc-substituted nickel ferrite nanoparticles, Journal of Superconductivity and Novel Magnetism 27(2), 2014, 547-553.
- [13] M.A. Gabal, M. Reda, El-Sishtawy and Y.M. Al Angari, Structural and magnetic properties of nanocrystalline Ni–Zn ferrites synthesized using egg-white precursor, Journal of Magnetism and Magnetic Materials 324(14), 2012, 2258-2264.
- [14] A.D. Sheikh and V.L. Mathe, Anomalous electrical properties of nanocrystalline Ni–Zn ferrite, Journal of Materials Science 43(6), 2008, 2018-2025.
- [15] L. Vegard, Die konstitution der mischkristalle und die raumfüllung der atome, Zeitschrift fur Physik5(1), 1921, 17-26.
- [16] Alex Goldmann, m, Modern Ferrite Technology (Springer, New York, 2006).

# Volume No.07, Special Issue No.02, February 2018

#### www.ijarse.com

ISSN: 2319-8354

- [17] R.D. Shannon, Revised effective ionic radii and systematic studies of interatomic distances in halides and chalcogenides, ActaCrystallographica, A32, 1976, 751.
- [18] K.E. Sickafus, and J.M. Wills, Structure of Spinel, Journal of American Ceramic Society 82(12), 1999, 3279-3292.
- [19] T.K. Gupta and R.L. Coble, Sintering of ZnO:I, Densification and Grain Growth, Journal of American Ceramic Society 51(9), 1968, 521-525.
- [20] Raul Valenzula, Magnetic Ceramics (Cambridge Press, 1994).
- [21] T.J. Shinde, A.B. Gadkari and P.N Vasambekar, DC resistivity of Ni–Zn ferrites prepared by oxalate precipitation method, Materials Chemistry and Physics 111(1), 2008, 87.
- [22] A.K.N. AktherHossain and M.L. Rahman, Enhancement of microstructure and initial permeability due to Cu substitution in Ni<sub>0.5-x</sub>Cu<sub>x</sub>Zn<sub>0.5</sub>Fe<sub>2</sub>O<sub>4</sub> ferrites, Journal of Magnetism and Magnetic Materials 323(15), 2011, 1954-1962.
- [23] S.S. Bellad, S.C. Watawe, A.M. Shaikh, B.K. Chougule, Cadmium substituted high permeability lithium ferrite, Bulletin of Materials Science 23(2), 2000, 83-85
- [24] L. Neel, Magnetism and Local Magnetic Field, Annals of Physics 3, 1948, 137.
- [25] D. Venkatesh, M.S.R. Prasad, B.R. Babu, K.V. Ramesh and K. Trinath, Effect of Sintering Temperature on the Micro Strain and Magnetic Properties of Ni-Zn Nanoferrites, Journal of Magnetics 20(3), 2015, 229-240.
- [26] M.S.R. Prasad, B.B.V.S. Prasad and B.R. Babu, Magnetic, structural and dc electrical resistivity studies on the divalent cobalt substituted Ni–Zn ferrite system, International Journal of Modern Physics B 29, 2015, 1550067(1-20)
- [27] C.P. Rana, J.S. Bajal and P. Kishan, Electrical conductivity of Ni 瑕Zn ferrites doped with Ti<sup>4+</sup> ions, Journal of Less Common Metals 106, 1985, 257-261.
- [28] PrinyaSainamthip and V.R.W. Amarkoon, Role of Zinc Volatilization on the Microstructure Development of Manganese Zinc Ferrites, Journal of American Ceramic Society 71, 1988, 644-648.
- [29] L.G. Van Uitert, High-Resistivity Nickel Ferrites—the Effect of Minor Additions of Manganese or Cobalt, Journal of Chemical Physics, 24(2), 1956, 306.
- [30] E. Rezlescu, L. Sachelariea and N. Rezlescu, Influence of copper ions on the structure and electromagnetic properties of MgZn ferrite, Journal of Optoelectronics and Advanced Materials 8(3), 2006, 1019-1022.
- [31] I.H. Gul, W. Ahmed and A. Maqsood, Electrical and magnetic characterization of nanocrystalline Ni–Zn ferrite synthesis by co-precipitation route, Journal of Magnetism and Magnetic Materials 320(3), 2008, 270-275.
- [32] A.K. Nikumbh, The formation, structural, electrical, magnetic and Mössbauer properties of ferrispinels,  $Cd_{1-x}Ni_xFe_2O_4$ , Journal of Materials Science 37(3), 2002, 637-647.